3D DESIGN OF THE IPHI RFQ CAVITY

P. Balleyguier, CEA Bruyères-le-Châtel, France

Abstract

Starting from 2D Superfish-based simulations, we studied the IPHI RFQ cavity from a 3D resonator point of view. The task was to give dimensions for a complete 3D mechanical design. This has been done by some analytical developments and localized constant models. Many 3D simulations were made with MAFIA, either to confirm some theoretical predictions or to give an accurate dimension for some localized details. Among the many questions studied were: synthesis of the required voltage law, RFQ ends, studying resonant coupling, RF losses, peak field, dipolar stabilizer rods,...

1 INTRODUCTION

The IPHI RFQ [1] is a 5 MeV high current (100 mA CW) proton accelerator. It is 8 m long, and will be fed by two 1.3 MW klystrons. It was designed in order to minimize particle losses and to keep the peak field level below 1.7 Kilpatrick (at 352 MHz). This led to variable aperture and voltage along the cavity. The design of the 2D cross section was performed with Superfish by R.Ferdinand: at each position, the cell area was adjusted in order to obtain a certain frequency resonance f_{2D} with a given aperture r_0 (fig. 1).

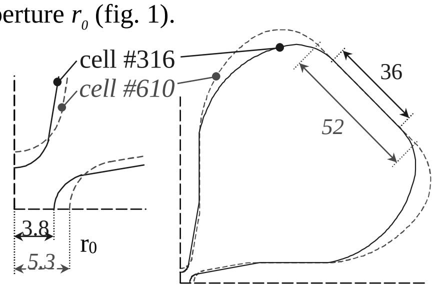

Fig. 1. RFQ cross-sections at two different locations.

2 RFQ ENDS

At both ends of an RFQ, undercuts must be performed in the vanes in order to close the magnetic field lines. Like any mechanical modification, the vane undercut causes *a priori* a local mismatch and then an unwanted frequency shift, compared to the cross-section frequency f_{2D}. The absolute detuning Δf is expected to depend on the relative importance of the vane end compared to the RFQ half-length L (the RFQ is assumed to be symmetrical with respect to its mid-length cross-section). Simulations confirmed that, for a given vane-end shape, the product $L\times\Delta f$ (in m.MHz) is roughly constant and characterizes the vane-end mismatch. This quantity can be computed from two simulations (a short RFQ, e.g. L=200 mm, and a pure 2D run) with identical transverse grids, because MAFIA frequencies are very 'mesh-sensitive'.

In the design process, detuning is canceled by adjusting the undercut length. MAFIA simulations (including the adaptation section) were performed for this purpose. As the resolution is still rather coarse, an adjustment is necessary during the fabrication. This will be done by re-machining the end plate, rather than modifying the vane themselves (fig. 2). According to simulations, the adjustment range is ±0.550 m.MHz.

Stabilizer rods will be provided to avoid mixing between dipolar and accelerating modes. Their position are set not to perturb the accelerating mode frequency.

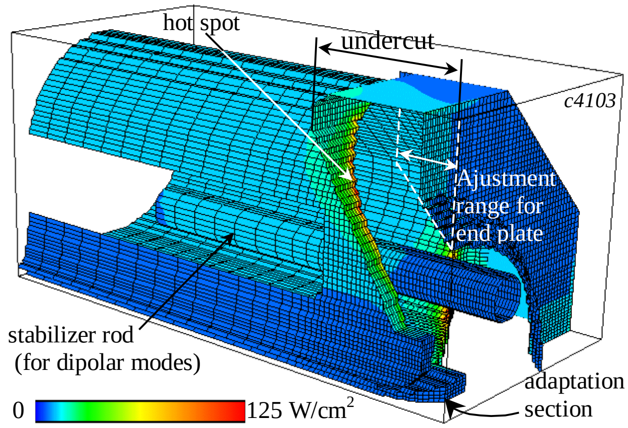

Fig. 2. Losses in IPHI RFQ input, computed with 'old' MAFIA: actually, the hot spot is still underestimated.

Local RF heat is a major concern in a CW high power RFQ like ours. A fine study showed that computed peak losses were sometimes underestimated by a folding factor 4. A new MAFIA version giving more realistic values resulted from this study [2]. Unfortunately, this loss enhancement occurs in regions that were already critical (fig. 2). A thermal analysis has been carried out by M.Painchault and J.Farjon [3], and it seems like that the copper elastic limit could be overtaken at certain spots. But the conclusions are not clear because transferring data between RF and thermal codes causes many problems. Further works are currently underway on this topic.

3 VOLTAGE LAW

To obtain a given non-constant voltage law V(z), we showed that the local frequency resonance must be shifted according to:

$$\frac{\Delta f(z)}{f_0} = \frac{1}{2}\left(\frac{\lambda}{2\pi}\right)^2 \frac{V''(z)}{V(z)}. \qquad (1)$$

Proof: each slice of the RFQ owns its frequency resonance $\omega(z)$ but is forced to resonate at the global RFQ frequency ω_0. So, it behaves like a slice of a uniform RFQ (with the same local cross-section) that would be driven at a HOM frequency ($\omega_p=\omega_0$) such as: $(\omega_0/c)^2 = (\omega(z)/c)^2+(p\pi/L)^2$. L is the length of the uniform RFQ, p is the longitudinal mode order. In such a mode, the transverse voltage depends on z as: $V(z)=V_0\cos(p\pi z/L)$.

Assuming $\Delta f \ll f_0$, eq.1 is derived by differentiating twice the last equation and combining it with the previous one.

Eq.1 requires that no second order discontinuities would appear in V(z). In other words, there should be no angles in the curve. From the opposite point of view, eq. 1 shows that any local mismatch causes a curvature in the voltage law.

In our RFQ, the voltage law is defined by a spline function that is twice derivable. The local frequency shift *Δf(z)* derived from eq.1 (fig. 3) was taken into account in the cross-section design: f_{2D} is not constant along the RFQ. As variations of aperture already imposes a continuously varying cross-section along the RFQ, including *Δf(z)* in the early design does not further complicate the structure. The cavity will be equipped with tuning plungers (every 250 mm in each quadrant), but only to compensate residual defaults: their adjusting range is only ± 1MHz.

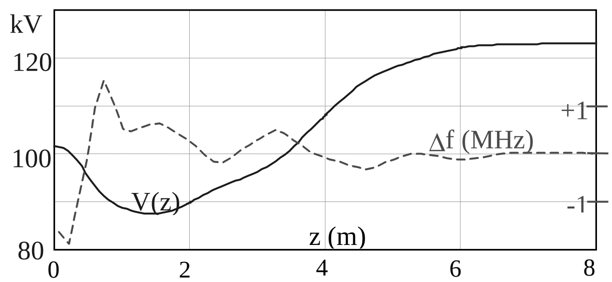

Fig. 3. Required voltage law and associated local Δf.

4 RESONANT COUPLING

A single-segment 8-m long RFQ would be very unstable because the longitudinal HOMs are very close in frequency from the accelerating mode. So, the cavity was split into four 2-m segments, and we adopted the LEDA resonant coupling technique with intervane gaps and coupling plate between contiguous segments [4]. The principle is to build a compensated structure, analogously to the π/2 structure in coupled cavity linacs (CCL), in which upper and lower next modes are equally separated in frequency from the operating mode.

The study of the segment ends is very similar to the case of RFQ extremities, except for the intervane gap. To design this gap, we first calculated the required 4-vane coupling capacity from A.Pisent's [5] formula :

$$C_{gap} = \left(\frac{\lambda}{2\pi}\right)^2 \frac{4C'}{\ell}, \qquad (2)$$

C' being the lineic capacity of the RFQ cross section (about 120 pF/m), ℓ being the segment length. Then, the gap thickness was determined from local electrostatic simulations of vane end tips. As first calculated gaps (3.5 mm) induced a rather important perturbation on the axis field, the coupling capacity surface was reduced by lowering the overhang height from 30 to 25 mm. For a given C_{gap}, this permitted to reduce the gap to 2.2 mm.

Splitting the RFQ into segments gives a better longitudinal stability. But then, how to prevent the compensated structure from "fighting" against the desired non-constant voltage? The solution is to bend the V(z) curve to horizontal at each gap, so that each segment can be seen as an independent RFQ with a perfect magnetic boundary condition at the coupling gap. It is done by a convenient mismatch on either side of the gap, depending on the local V(z) slope (fig. 4). As a consequence, the undercuts on either side of the coupling plate are slightly asymmetrical (fig. 5).

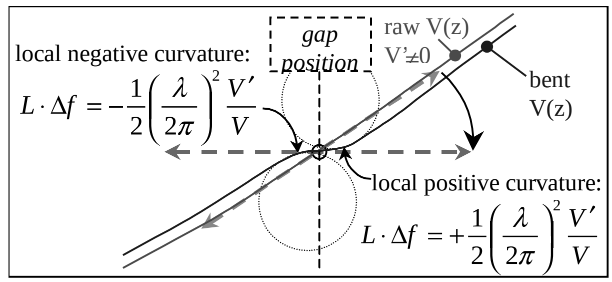

Fig. 4. Local bend of V(z) to get a horizontal tangent

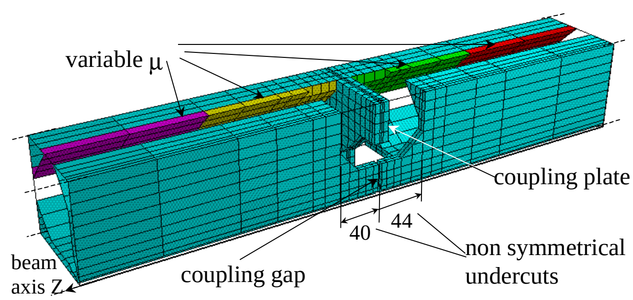

Fig. 5. Resonant coupling (as simulated in section 5).

5 SIMULATION

To confirm the principles exposed in previous sections, we simulated with MAFIA a global 8-m RFQ with a poor resolution in order to keep a reasonable number of points (about 25000). Because of the coarse resolution, it was not possible to represent a continuously varying volume in the cross-section to reproduce the *Δf(z)* curve plotted on figure 3. Instead of that, we simulated a small magnetic region in the cross section (fig. 6a) with a continuously adjustable permittivity. The link between μ and Δf was established from 2D simulations (fig. 6b), allowing to translate *Δf(z)* into *μ(z)*. The corresponding 3D cavity was then simulated, and the resulting V(z) curve fitted exactly with the required one.

Then, three resonant couplings were introduced to split the simulated cavity into four 2-m segments. Originally, the segment ends were simply matched in frequency by adjusting the undercuts (just like in RFQ input). The structure tries to compensate the non-constant V(z) curve, and voltage steps appear at coupling gaps. To get rid of those steps, the segment ends were conveniently detuned (according to equation in fig. 4) resulting in non-symmetrical undercuts. Except for a narrow drop at the gap itself, the final V(z) is very close to the goal (fig. 7) .

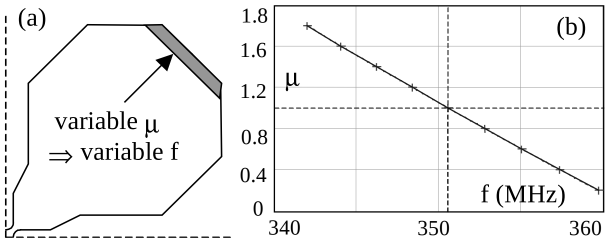

Fig. 6. Simulating Δf with a variable μ zone.

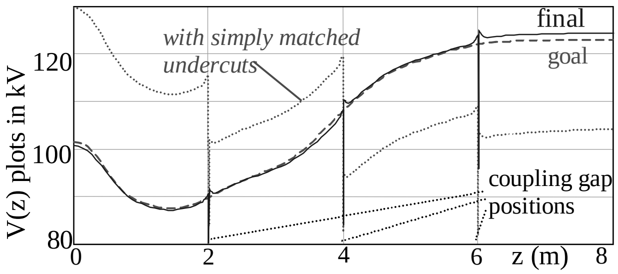

Fig. 7. Simulation of a segmented RFQ with a non-constant voltage law.

6 PEAK FIELD ON VANE ENDS

Dividing the RFQ into segments has another drawback: electric field increases at the vane end corners (fig. 8b) [6]. As a first approximation based on cylindrical capacities, the field enhancement factor K is linked to the local curvature radius r and to the inter-vane half-distance d by: $K \approx 1+d/6r$. For example, typical IPHI RFQ values ($r=0.75$ *mm*, $d=1.17$ *mm*) lead to an unacceptable local field: *2.38 Kilp* (fig. 8b). According to the experimental link between peak-voltage and spark-rate measured on the CRITS RFQ [7] (*4.5 decade/Kilp.*), this 40 % field increase would result in a 1700 folding factor on local spark rate.

Increasing r to obtain a reasonable peak field ($K=1.10$, for example, which already quadruples the local spark rate) leads to unrealistic radius values ($r > 17$ *mm*). So, we rather increased the radius locally by an elliptical corner. Large r values can be obtained by increasing the longitudinal half-axis a and reducing the transverse axis b (fig. 8c). But when the ellipse gets too flat, the peak field shifts toward the other extremity of the ellipse arc. So, all of this have been checked by electrostatics simulations. A good compromise was found with the following half-axis's: $a=2$ *mm*, $b= 0.75$ *mm.*

On the other hand, such elliptical corners slightly enforces the on-axis field drop due to the coupling gap. Studies were carried out in order to estimate the influence of such gaps in terms of particle loss. With a gap positioned so that the field vanishes when the bunch center crosses it (according to L.Young's advice), R.Duperrier showed with TOUTATIS [8] that 2.2 mm gaps should have no noticeable effect on particle loss.

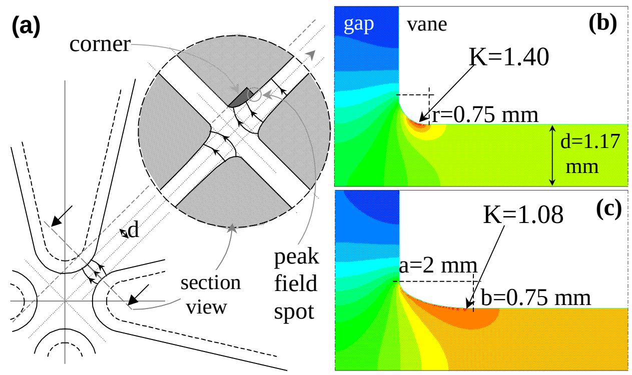

Fig. 8. Electrical field enhancement on vane ends: round corner (+40%), optimized elliptical corner (+8%).

7 CONCLUSION

Though accurate global 3D RFQ simulations are still far from today's computer capacities, most of the IPHI RFQ' details have been simulated either by analytical models or local simulations (including 2D cross-section computations). MAFIA was intensively used for this purpose, and also for validating concepts on coarse grid global models. Other elements are still to study, like RF input ports.

REFERENCES

[1] R. Ferdinand et al., "Status report on the IPHI RFQ", this conference (Linac2000, Monterey).

[2] P. Balleyguier et al., "Improvement in 3D computation of RF-losses in resonant cavities", this conference (Linac2000, Monterey).

[3] M. Painchault, "Main steps for fabrication of the IPHI RFQ", this conference (Linac2000, Monterey).

[4] J. Browman et al., "Coupled RFQs as Compensated Structures", Linac90, Albuquerque, p. 70.

[5] A.Pisent, "Equivalent Lumped Circuit Study for the Field Stabilization of a Long Four-Vanes RFQ", Linac98, Chicago, p.968.

[6] P. Balleyguier, " Peak field studies in the IPHI RFQ", HPPA workshop, Aix-en-Provence, 1999.

[7] G. Bolme et al., "Sparking-Rate and Breakdown-Protection Studies with a CW RFQ Linac", Particle Accelerator Conference, New York, 1999, p.1447.

[8] R. Duperrier et al., "Toutatis, the CEA-Saclay RFQ code", this conference (Linac2000, Monterey).